Int. J. Solids Structures Vol. 29, No. 2, pp. 197–213, 1992
Printed in Great Britain

0020-7683/92 $3.00 + .00

A RECURSIVE CONCENTRIC CYLINDER MODEL FOR COMPOSITES CONTAINING COATED FIBERS

MUZAFFER SUTCU
GE Corporate Research and Development, Schenectady, NY 12301, U.S.A.

(*Received* 18 *July* 1990; *in revised form* 4 *April* 1991)

Abstract—A simple recursive algorithm which considers only two concentric cylinders at a time is presented in order to calculate five effective elastic constants and two linear thermal expansion coefficients for a uniaxially aligned composite which contains an arbitrary number of coatings on its fibers. The micro stresses and the micro displacements are determined under combined applied radial and axial load and temperature change. During composite fabrication, each coating can be processed at a different temperature so that the zero-thermal-stress temperature is not unique for the composite. When layer properties vary with load and temperature, an incremental recursive analysis can be done by adjusting the zero stress temperatures at each step in order to induce initial stresses. The material for each constituent is assumed to be transversely isotropic with its axis oriented in the fiber direction. Approximate expressions for the equivalent axial and the transverse shear moduli are given in order to replace effectively two concentric cylinders with a single homogeneous cylinder. It is shown that the effective shear modulus of two concentric cylinders measured from a torsion test does not correspond to any of the effective shear moduli. The three remaining effective elastic constants and the two thermal expansion coefficients for two cylinders are the same as those given for a two-phase composite. The recursive method is applied to a titanium matrix composite reinforced with CVD SiC filaments (AVCO SCS-6). The inhomogeneous structure of the fiber is shown to influence the stress distribution and the composite elastic properties.

INTRODUCTION

A recursive elastic solution method can be outlined for uniaxial composites similar to the way in which the composites are processed. The fiber bundles in a composite are coated prior to the introduction of the matrix material. If multiple coatings are used, then each layer may be introduced at a different temperature; the final step being the processing of the matrix at its own processing temperature.

In general, the microstresses are non zero within the multiple coatings at the matrix processing temperature. Therefore, a single composite thermal set temperature may not exist for all the constituents. The stress distribution becomes even more complex when intrinsic stresses are introduced during manufacturing. Deposition stresses can arise from CVD, PVD or plasma-spraying processes.

The approach in this paper is as follows. Each coating layer is approximated as a hollow cylinder, the innermost fiber being solid. We begin with the innermost two cylinders and then move outwards, while replacing the coating and the fiber assembly underneath with an equivalent homogeneous transversely isotropic solid cylinder at each step (Figs 1 and 2). The effective elastic properties of this equivalent cylinder are calculated from the well known expressions in the literature (Christensen, 1979; Hashin, 1979) which are given for a two-phase composite. This process is repeated until all the coatings are assembled into the main fiber. The final step is the addition of the matrix.

After this replacement procedure, the stress determination problem for multiple coatings is essentially reduced to the problem of a single homogeneous transversely isotropic fiber. The boundary conditions on the matrix govern the stresses in the matrix and the effective stresses and the effective displacements in the fibers. The effective stresses and the effective displacements are defined only for the equivalent homogeneous cylinder; however, the resulting interface stress and the displacement values are actual quantities and act as boundary conditions for the next concentric cylinder assembly underneath. The matrix layer is ignored for the next solution step, because its effect is built into the boundary conditions. In this manner, the analysis progresses inwards until the innermost fiber is utilized. Thus, all microstresses and micro-displacements are calculated.

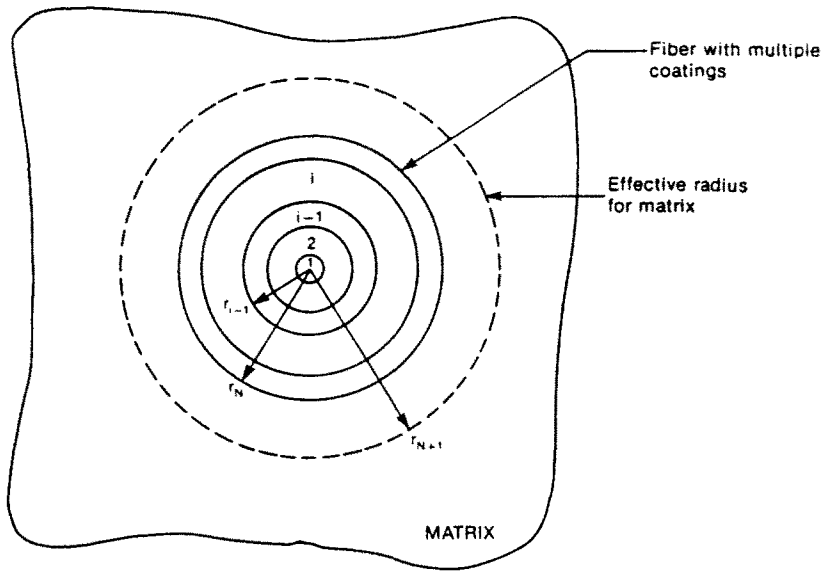

Fig. 1. The fiber is composed of N concentric layers. The matrix is approximated as a cylindrical jacket around the fiber and numbered $N+1$. The effective radius r_{N+1} for matrix is calculated from (3). Layer i is free of residual stress at temperature T_i in the absence of the outer layers. The innermost core is numbered 1.

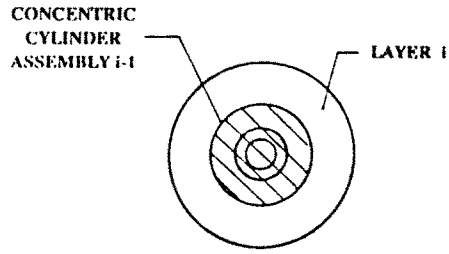

Fig. 2. Determination of the effective elastic constants in a recursive manner involves the replacement of the inner layers (shaded region) with an equivalent homogeneous transversely isotropic fiber and subsequently the addition of another layer.

BACKGROUND

The derivation of elasticity solutions for concentric cylinders is straightforward. A four-concentric-cylinder model is presented by Mikata and Taya (1985) for axisymmetric deformations. The four-cylinder model in Mikata and Taya (1985), together with a two-cylinder model, are used in Mikata *et al.* (1987) to determine the thermal residual stresses at two different steps during the fabrication of a Ni-coated carbon fiber composite. Some typographical errors in Mikata and Taya (1985) are corrected in Mikata *et al.* (1987). The solution for pure shear loading of two concentric cylinders is given by Christensen (1979), assuming unit shear loading of the composite at infinity. The solution in Christensen becomes valid for transversely isotropic constituents, if we make the following slight change in the definition of the elastic constants:

$$\eta = 1 + 2\mu_{23}/K_{23} \tag{1a}$$

$$\eta_m = 1 + 2\mu_{23,m}/K_{23,m} \tag{1b}$$

$$\eta_f = 1 + 2\mu_{23,f}/K_{23,f}. \tag{1c}$$

The notation in (1a)–(1c) is that of Christensen (1979) and is different than that of this paper. The quantities η, η_m and η_f are the elastic constants of the composite (outer cylinder), the matrix (middle layer) and the fiber (inner core) respectively, and appear in expression

(3.14) in Christensen for the in-plane shear modulus. The single-valued transverse shear modulus in Christensen is derived for composites made with isotropic constituents. The extension to the case of the transversely isotropic constituents is done by simply redefining the elastic constants η, η_f and η_m as done in (1a)–(1c).

Two recent papers by Pagano and Tandon (1988, 1989) present quite general non-axisymmetric solutions for an assembly of three concentric cylinders. The solutions in Pagano and Tandon are based on Pagano's original paper (1972).

A multiple-coated uniaxially aligned fiber composite has five independent effective elastic constants and two linear thermal expansion coefficients, provided each phase is either isotropic or transversely isotropic with its axis aligned along the fiber direction. Exact predictions for the four elastic constants of a two-phase composite, namely the axial Young's modulus E^A, the axial Poisson's ratio ν^A, the axial shear modulus G^A, the transverse bulk modulus k, are given by Christensen (1979) for isotropic constituents (with reference to other literature) and by Hashin (1979) for transversely isotropic constituents. The expressions for the two effective linear thermal expansion coefficients are given in Christensen or Hashin for isotropic constituents; however, with some work the reader can obtain the transversely isotropic case.

Close upper and lower bound values for the remaining fifth elastic constant, namely the in-plane shear modulus G^T, are provided by Hashin (1979) for a two-phase composite. A single valued in-plane shear modulus is given in Christensen (1979) for a two-phase composite.

The expressions given in the literature for the three effective elastic constants E^A, ν^A, k and the two thermal expansion coefficients can be used effectively to replace two concentric cylinders with an equivalent homogeneous solid cylinder, although these expressions were derived for a two-phase composite where the inner phase is finely dispersed within the outer layer. The expressions for the remaining two elastic constants, namely the in-plane and the axial shear moduli G^T and G^A, which are provided by Christensen ((1979) and Hashin (1979), are valid only when the inner phase is in the form of finely distributed cylinders. These expressions are not accurate for the replacement of two concentric cylinders with a homogeneous equivalent. More accurate, but still approximate expressions for the effective axial and in-plane shear moduli are derived elsewhere and will be given here for the recursive algorithm. It should be noted that the overall torsional shear modulus is different than the effective axial shear modulus for concentric cylinders. This is discussed in Appendix C of this paper.

EFFECTIVE ELASTIC CONSTANTS

As mentioned earlier, a uniaxially reinforced composite is considered to be transversely isotropic with five effective constants and two linear thermal expansion coefficients. The axial and the transverse Young's moduli are denoted by E^A and E^T, respectively. The lateral deformation in the plane of the isotropy is governed by ν^A when load is applied in the axial direction, and by ν^T when load is applied in the plane of the isotropy. When shear stresses are applied parallel to the material axis, the governing shear modulus is denoted by G^A. The remaining shear modulus G^T governs the response when the shear stresses are applied in the plane of the isotropy and is related to the Young's modulus E^T and the Poisson's ratio ν^T in a manner similar to the isotropic materials. Another elastic constant which is dependent on the other five independent elastic constants is the transverse bulk modulus k (not to be confused with the bulk modulus K for isotropic materials) and given by Hashin (1979)

$$2k = E^T/(1+\nu^T-2(\nu^A)^2E^T/E^A). \tag{2}$$

For incompressible materials, the transverse bulk modulus k is infinitely large. A transversely isotropic material possesses two linear thermal expansion coefficients. The expansion coefficients in the axial and transverse directions are denoted by α^A and α^T, respectively.

The layers are numbered, beginning with the innermost fiber (Fig. 1). Innermost fiber is numbered 1, the adjacent coating is numbered 2, the next layer 3, etc.; finally the matrix being numbered $N+1$. Excluding the innermost fiber and the matrix phases, the number of coatings is accordingly $N-1$. The outer radius of each coating layer is denoted by r_i, where the subscript i denotes the layer number. Thus, the outer radius of the innermost fiber is r_1. An effective radius for the matrix is calculated from the specified matrix volume fraction V^m as follows:

$$r_{N+1} = r_N\sqrt{1-V_m} \tag{3}$$

where r_N is the radius of the fiber including the thickness of all the layers of the multiple coatings.

In general, a superscript "e" will indicate that the symbol refers to an effective property. If a quantity has the superscript "e", such as E_i^{Ae}, then the subscript i will refer to the number of coatings which have been incorporated into that property. On the other hand, the symbol E_i^A without the superscript "e" refers to the material property of the ith layer.

The effective properties for layer 1 are set to be equal to the respective properties of the innermost fiber. For two or more layers, $N>1$, the effective properties are given below. The range of the index i is, $i=2, N+1$. First, we define a number of quantities for mathematical convenience:

$$f_i = (r_{i-1}/r_i)^2 \tag{4}$$

$$\bar{E}_A = f_i E_{i-1}^{Ae} + (1-f_i)E_i^A. \tag{5}$$

The term f_i in (4) is the relative volume fraction of the $(i-1)$th cylinder with respect to the ith layer.

Transverse bulk modulus:

$$k_i^e = \frac{k_i(k_{i-1}^e + G_i^I)(1-f_i) + k_{i-1}^e(k_i + G_i^I)f_i}{(k_{i-1}^e + G_i^I)(1-f_i) + (k_i + G_i^I)f_i}. \tag{6}$$

Axial Young's modulus:

$$E_i^{Ae} = \bar{E}_A + \frac{4(v_i^{Ae}{}_{-1} - v_i^A)^2 f_i(1-f_i)}{(1-f_i)/k_{i-1}^e + f_i/k_i + 1/G_i^I}. \tag{7}$$

Axial Poisson's ratio:

$$v_i^{Ae} = v_i^A(1-f_i) + v_{i-1}^{Ae}f_i + \frac{(v_{i-1}^{Ae} - v_i^A)(1/k_i - 1/k_{i-1}^e)f_i(1-f_i)}{(1-f_i)/k_{i-1}^e + f_i/k_i + 1/G_i^I}. \tag{8}$$

The effective axial and the in-plane shear moduli of two concentric solid cylinders are derived by replacing a concentric cylinder assembly with an equivalent transversely isotropic homogeneous cylinder embedded in an elastic composite and subjecting the composite to homogeneous boundary conditions. If the inner phase is finely dispersed in the outer layer, then the expressions provided by Christensen (1979) and Hashin (1979) which are given in Appendix B should be used instead of the expressions given below.

Axial shear modulus:

$$G_i^{Ae} = G_i^A + 2f_i(G_{i-1}^{Ae} - G_i^A)/(1+f_i). \tag{9}$$

Transverse shear modulus:

$$G_i^{Te}/G_i^T - 1 = (-B \pm \sqrt{B^2 - AC})/A \tag{10}$$

where the quantities A, B, and C are given in Appendix A in terms of the elastic properties and volume fractions of the inner and the outer layers. Numerical experimentation with the expressions in (10) and (A1)–(A13) shows that the "+" sign is valid when the inner phase is stiffer ($\eta_2 \geqslant 1$, $G_{i-1}^{Te} > G_i^T$) and the "−" sign is valid when $\eta_2 < 1$, $G_{i-1}^{Te} < G_i^T$.

Thermal expansion coefficients do not pose any difficulties and are given below.

Axial thermal expansion coefficient:

$$\begin{aligned}
\alpha_i^{Ae} &= [f_i E_{i-1}^{Ae} \alpha_{i-1}^{Ae} + (1-f_i) E_i^A \alpha_i^A]/\bar{E}_A + (p_1^A + p_2^A)/q \\
p_1^A &= 4(\alpha_{i-1}^{Ae} - \alpha_i^A) f_i (1-f_i)(\nu_{i-1}^{Ae} - \nu_i^A) G_i^T k_i k_{i-1}^e [E_i^A \nu_i^A (1-f_i) + E_{i-1}^{Ae} \nu_{i-1}^{Ae} f_i]/\bar{E}_A \\
p_2^A &= 4(\alpha_{i-1}^{Te} - \alpha_i^T) f_i (1-f_i)(\nu_{i-1}^{Ae} - \nu_i^A) G_i^T k_i k_{i-1}^e \\
q &= \bar{E}_A [k_i k_{i-1}^e + G_i^T (k_i (1-f_i) + k_{i-1}^e f_i)] + 4 G_i^T k_i k_{i-1}^e (\nu_{i-1}^{Ae} - \nu_i^A)^2 f_i (1-f_i).
\end{aligned} \tag{11}$$

Transverse thermal expansion coefficient:

$$\begin{aligned}
\alpha_i^{Te} &= \alpha_i^T + (p_1^T + p_2^T)/q \\
p_1^T &= (\alpha_{i-1}^{Te} - \alpha_i^T) k_{i-1}^e f_i [\bar{E}_A (k_i + G_i^T) + 4(1-f_i) k_i G_i^T (\nu_i^A - \nu_{i-1}^{Ae})] \\
p_2^T &= (\alpha_{i-1}^{Ae} - \alpha_i^A) f_i [\bar{E}_A (k_i + G_i^T) k_{i-1}^e \nu_{i-1}^{Ae} + 4(1-f_i) G_i^T k_i k_{i-1}^e \nu_i^A \nu_{i-1}^{Ae} (\nu_i^A - \nu_{i-1}^{Ae}) \\
&\quad - E_{i-1}^{Ae} [G_i^T (k_{i-1}^e \nu_{i-1}^{Ae} f_i + k_i \nu_i^A (1-f_i)) + k_i k_{i-1}^e (\nu_i^A (1-f_i) + \nu_{i-1}^{Ae} f_i)]].
\end{aligned} \tag{12}$$

For the reader who is interested in the properties of two concentric cylinders only, the above complicated set of subscripts and superscripts can be simplified drastically, if we keep in mind that combination of the subscript $i-1$ and the superscript "e" refer to the properties of the inner cylinder, whereas the subscript i refers to the properties of the outer cylinder (Fig. 2). The relative volume fraction f_i in (4) is excluded from this rule.

In the above set of equations we gave the expressions for five independent elastic constants and two thermal expansion coefficients. The remaining elastic constants are determined from

$$E^T = 4kG^T/(k + m^* G^T) \tag{13a}$$

$$\nu^T = (k - m^* G^T)/(k + m^* G^T) \tag{13b}$$

$$m^* = 1 + 4k(\nu^A)^2/E^A. \tag{13c}$$

For the sake of simplicity, we dropped the superscripts "e" and the subscripts i.

STRESSES AND DISPLACEMENTS UNDER AXISYMMETRIC LOADING

In the previous section we indicated that the determination of the effective elastic properties is an outwards process, namely the successive replacement of the inner concentric cylinders with their equivalent homogeneous solid cylinders until we arrive at the matrix phase. The determination of the displacements and the stresses is similar, except now we move inwards. With this recursive approach, we need to solve a two-concentric-cylinder model at each step (Fig. 2). The solution for a two-concentric-cylinder model can be found easily: see Lekhnitskii (1981) or Mikata and Taya (1985) among others (see the latter for the governing equations).

The symbol T_i denotes the temperature at which the ith layer has been introduced over the inner concentric cylinders in a stress-free manner. In other words, the ith coating is free of thermal stresses at the temperature T_i, in the absence of the outer coating layers and the matrix. The temperature T_i, called the "set" temperature, is the zero thermal stress temperature for the two-concentric-cylinder assembly. From a computational point of view,

the temperature T_i is a convenient reference for the two-concentric-cylinder assembly from which the displacements can be calculated by applying the displacement boundary conditions at the interface. However, from a practical point of view, it is confusing to have the displacements of each layer with respect to a different temperature T_i in the final solution for all the concentric layers. To remedy this situation, (i) we solve the two concentric cylinder model by assuming that the thermal strains and the displacements are zero at the reference temperature T_i; and (ii) subsequently, we subtract the thermal strains and the thermal displacements so that all layer strains and displacements are calculated from the current temperature T, at which the composite is being used. Note that the stresses are not affected by this procedure. Combining these two steps, the displacements and the strains are given below with respect to the current temperature T.

Displacements

$$u^r = D_1 r + D_2/r - u^{rt} \tag{14}$$

$$u^\theta = 0 \tag{15}$$

$$u^x = D_3 x - u^{xt} \tag{16}$$

where

$$u^{rt} = \alpha^T (T - T_i) r \tag{17}$$

$$u^{xt} = \alpha^A (T - T_i) x. \tag{18}$$

Lower case "t" is used as a superscript to distinguish thermal displacements.

Strains

$$\varepsilon^{rr} = u^{r,r} = D_1 - D_2/r^2 - \alpha^T (T - T_i) \tag{19}$$

$$\varepsilon^{\theta\theta} = u^r/r = D_1 + D_2/r^2 - \alpha^T (T - T_i) \tag{20}$$

$$\varepsilon^{xx} = u^{x,x} = D_3 - \alpha^A (T - T_i). \tag{21}$$

All shear strain components are zero.

Stresses

$$\sigma^{xx} = C_{11}(D_3 - e^x) + 2C_{12}(D_1 - e^r) \tag{22}$$

$$\sigma^{rr} = 2k(D_1 - e^r) - 2G^T D_2/r^2 + C_{12}(D_3 - e^x) \tag{23}$$

$$\sigma^{\theta\theta} = 2k(D_1 - e^r) + 2G^T D_2/r^2 + C_{12}(D_3 - e^x) \tag{24}$$

where

$$C_{11} = E^A + 4k(\nu^A)^2 \tag{25a}$$

$$C_{12} = 2k\nu^A \tag{25b}$$

$$e^r = \alpha^T (T - T_i) \tag{26a}$$

$$e^x = \alpha^A (T - T_i). \tag{26b}$$

For the sake of simplicity we did not use superscripts or subscripts in (14)–(26b) to

distinguish the inner and the outer cylinders. Similar to the previous section, we will designate the properties of the inner cylinder by a combination of the superscript "e" and the subscript $i-1$. The properties of the outer cylinder are denoted by the subscript i. The new terms in (14) and (16) include the radial and axial thermal displacements u^{rt} and u^{xt} respectively. The constants D_1, D_2 and D_3 are to be determined from the boundary conditions. The corresponding sets for the inner and outer cylinders are denoted by $D^e_{1,i-1}$, $D^e_{2,i-1}$, $D^e_{3,i-1}$, and $D_{1,i}$, $D_{2,i}$, $D_{3,i}$, respectively. The elastic constants for the inner and the outer cylinders $C^e_{11,i-1}$, $C^e_{12,i-1}$, and $C_{11,i}$, $C_{12,i}$ are expressed in terms of the previously defined elastic constants k, E^A and ν^A by adding the corresponding superscripts and the subscripts to (25a) and (25b). By a similar addition of the subscripts and superscripts the definition of the inner and the outer cylinder thermal strains e^{re}_{i-1}, e^{xe}_{i-1} and e^r_i, e^x_i can be obtained from (26a) and (26b).

Since the inner cylinder is a solid cylinder, the radial displacement u^{re}_{i-1} is zero at the center where $r = 0$. This condition leads to

$$D^e_{2,i-1} = 0. \tag{27}$$

Thus, the inner phase transverse shear modulus G^{Te}_{i-1} in (23) and (24) does not enter the calculations. Continuity of axial displacement at the interface at $r = r_{i-1}$,

$$u^x_i + u^{xt}_i = u^{xe}_{i-1} + u^{xte}_{i-1}, \tag{28a}$$

yields

$$D_{3,i} = D^e_{3,i-1}. \tag{28b}$$

Continuity of radial displacement at $r = r_{i-1}$,

$$u^r_i + u^{rt}_i = u^{re}_{i-1} + u^{rte}_{i-1}, \tag{29a}$$

gives

$$D_{1,i} r_{i-1} + D_{2,i}/r_{i-1} = D^e_{1,i-1} r_{i-1}. \tag{29b}$$

Continuity of radial stress at $r = r_{i-1}$,

$$\sigma^{rr}_i = \sigma^{rre}_{i-1}, \tag{30a}$$

gives

$$2k_i(D_{1,i} - e^r_i) - 2G^T_i D_{2,i}/r^2_{i-1} + C_{12,i}(D_{3,i} - e^x_i) = 2k^e_{i-1}(D^e_{1,i-1} - e^{re}_{i-1}) + C^e_{12,i-1}(D^e_{3,i-1} - e^{xe}_{i-1}). \tag{30b}$$

Radial applied stress on the outer surface at $r = r_i$,

$$\sigma^{rr}_i = \sigma^{rre}_i, \tag{31a}$$

gives

$$\sigma^{rre}_i = 2k_i(D_{1,i} - e^r_i) - 2G^T_i D_{2,i}/r^2_i + C_{12,i}(D_{3,i} - e^x_i). \tag{31b}$$

Axial applied stress at infinite distance

$$\sigma_i^{xx}(1-f_i)+\sigma_{i-1}^{xxc}f_i=\sigma_i^{xxc} \tag{32a}$$

gives

$$\sigma_i^{xxc}=f_i[C_{11,i-1}^{c}(D_{3,i-1}^{c}-e_{i-1}^{xc})+2C_{12,i-1}^{c}(D_{1,i-1}^{c}-e_{i-1}^{rc})] + (1-f_i)[C_{11,i}(D_{3,i}-e_i^{x})+2C_{12,i}(D_{1,i}-e_i^{r})]. \tag{32b}$$

As we change the subscript i from $N+1$ to 2, for each i we solve the five equations (28b), (29b), (30b), (31b) and (32b) for the five unknowns $D_{1,i}$, $D_{2,i}$, $D_{3,i}$, $D_{1,i-1}^{c}$ and $D_{3,i-1}^{c}$. This recursive process is initialized by using the applied axial stress σ^{ax} and the applied radial stress σ^{ar} on the composite:

$$\sigma_{N+1}^{xxc}=\sigma^{ax} \tag{33}$$

$$\sigma_{N+1}^{rrc}=\sigma^{ar}. \tag{34}$$

The effective stresses, the effective displacements and the effective elastic constants of the innermost cylinder are the same as the actual quantities. It should be noted that the quantity $D_{3,i}$ in (28b) is constant for all the phases and represents the actual axial composite strain as measured from the matrix set temperature T_{N+1}, under combined load and temperature change.

The recursive method is incorporated into a Fortran computer program so that parametric studies can be done easily using a range of realistic material property values.

CVD SiC FIBERS IN A TITANIUM MATRIX COMPOSITE

The material considered in this section is a titanium matrix composite reinforced with CVD SCS-6 SiC filaments which are manufactured by Textron (formerly AVCO). The effective elastic properties of the fiber by itself as well as those of the composite, together with the microstresses and the displacements, are calculated using the recursive cylinder approach. The matrix material is Ti-6Al-2Sn-4Zr-2Mo. Previous micromechanical work on this composite has been detailed by Nimmer *et al.* (1989). Detailed microstructure of the SiC fibers is given by Nutt and Wawner (1985); further microstructural information and property measurements are given by Brun and Borom (1989), Siemers *et al.* (1988) and DiCarlo (private communication), among others. SCS-6 filaments are produced by depositing β-SiC onto an approximately 36-μm-diameter carbon core up to a diameter of approximately 137 μm. The inner carbon core is isotropic and carefully chosen to match the thermal expansion of the SiC layer; however, the measurements of DiCarlo indicate that this may not be the case. Nevertheless, the influence of the core is not significant because of its relatively small radius and the volume fraction. On top of the SiC layer are introduced two layers of carbon-rich silicon carbide finish, each 1–1.5 μm thick. Thus, the final diameter of the fiber is approximately 142 μm. The two outside coatings show variation from batch to batch in their composition. The batch studied by Nutt and Wawner (1985) seems to contain preferentially oriented pyrolytic carbon in the first layer of the outside coatings, and the second layer is mostly isotropic carbon. However, other batches include some SiC on the outside as well as the inner layer (DiCarlo, private communication).

Our primary purpose is to demonstrate the usefulness and the capabilities of the recursive approach. Exact mechanical properties of the individual layers within the fiber, especially those of the outer coatings, can only be guessed from the microstructural observations. Because of the lack of proper material data the properties used in this section represent the best guess of this author and should be used with caution. Parametric studies (this will not be done here) can be done using a range of realistic material property values in order to gain some insight.

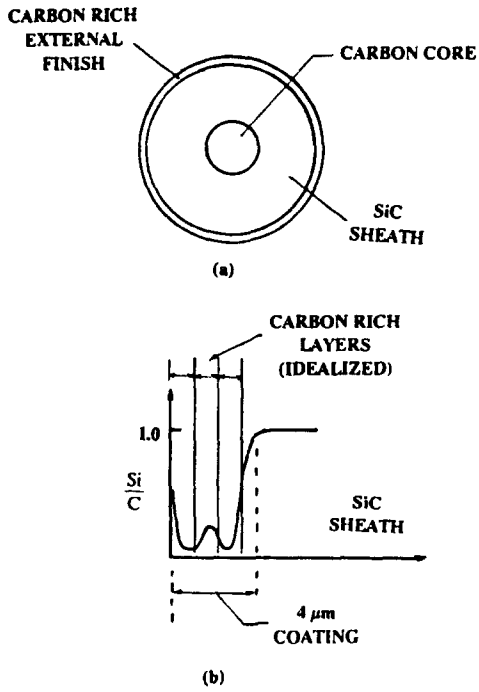

Fig. 3. The structure of the CVD SiC fiber. (a) Cross section of the fiber with carbon-rich coatings. (b) The composition of the external coating from DiCarlo (private communication). The ratio of Si to C in the outer fiber layer is plotted against the radial distance from the external surface of the fiber. The idealized model assumes that the coating region can be divided into three layers.

The idealized SiC fiber structure is shown in Fig. 3 and the assumed values for the constituent material properties are given in Tables 1 and 2. The material properties are assumed to be elastic and constant over the temperature range. Matrix volume fraction (V_m) is 0.72. Because of the presence of pyrolytic carbon we assume that the first of the

Table 1. Composite material data

Constituents i			Outer radius r_i (μm)	Relative volume fraction (f_i)	Young's mod. E_i^A (GPa)	Shear mod. G_i^T (GPa)	Thermal expansion α_i^A (1/°C × 10^6)	Set temp. (°C)
CVD	1	Carbon core	18	—	50	20.8	4.5	—
SiC	2	SiC sheath	68	0.070	430	179	4.5	1300
Fiber	3	Coat. 1	69	0.971	300	41.7	4.7	1300
	4	Coat. 2	70	0.972	400	83.3	4.5	1300
	5	Coat. 3	71	0.972	300	20.8	5.0	1300
Matrix	6	Ti-6Al-2Sn-4Zr-2Mo	134.2	0.280	95	36.5	11.0	820

All phases are isotropic except layers 3–5 (see Table 2).
All Poisson's ratios are 0.2, except $\nu_3 = 0.3$ for matrix.
Matrix volume fraction is $V_m = 0.72$.

Table 2. Material data for anisotropic layers 3–5 in Table 1

Property	Layer 3	Layer 4	Layer 5
E_i^T (MPa)	100	200	50
G_i^A (MPa)	68	118	40
ν_i^A	0.2	0.2	0.2
ν_i^T	0.2	0.2	0.2
k_i (MPa)	65	132	32
α_i^T (1/°C × 10^6)	5.0	4.5	5.0

Table 3. Calculated effective properties for the composite

Number of layers		Young's moduli GPa		Shear moduli GPa		Poisson's ratio		Thermal expansion ($1/°C \times 10^6$)	
	i	E_i^{Ae}	E^{Te}	G_i^{Ae}	G^{Te}	ν^{Te}	ν_i^{Ae}	α_i^{Ae}	α^{Te}
CVD SiC Fiber	2	403	307	158	114	0.349	0.20	4.50	4.50
	3	400	297	157	111	0.335	0.20	4.50	4.51
	4	400	294	156	110	0.330	0.20	4.50	4.51
	5	398	274	155	105	0.305	0.20	4.52	4.52
Matrix (Ti-6Al-2Sn-4Zr-2Mo)	6	180	126	51.8	46.9	0.337	0.268	7.09	9.58

For matrix phase, eqns (A14)–(A27) in Appendix B are used.

Table 4. Bounds on elastic constants (Hashin, 1979)

i	E_i^{Le}	E_i^{Ue}	G_i^{Le}	G_i^{Ue}	ν_i^{Le}	ν_i^{Ue}
2	372	367	154	150	0.222	0.212
3	352	347	145	142	0.223	0.213
4	346	341	142	140	0.223	0.213
5	310	306	127	125	0.226	0.216
6	130	128	50	48	0.326	0.312

Comparison with Table 3 shows that the effective moduli for two concentric cylinders are outside of the range defined by Hashin (1979).

The in-plane moduli calculated by recursive application of Christensen's value is within these bounds. Moduli are in GPa.

Table 5. Displacements and axial strains at $T = 20$ C and $T = 1020$ C

Layer i	$T = 20$ C			$T = 1020$ C		
	Radial disp. u_i' at $r = r_{i-1}$	Radial disp. u_i' at $r = r_i$	Axial strain $\varepsilon_i^{zz} \times 10^3$	Radial disp u_i' at $r = r_{i-1}$	Radial disp u_i' at $r = r_i$	Axial strain $\varepsilon_i^{zz} \times 10^3$
1	0.0000	−0.0129	−0.208	0.0000	0.0032	0.051
2	0.0129	−0.0091	−0.208	0.0032	0.0023	0.051
3	0.0344	0.0321	0.182	0.0118	0.0123	0.057
4	−0.0121	−0.0128	−0.208	0.00265	0.00284	0.051
5	0.0320	0.0269	−0.144	0.0126	0.0138	0.065
6	0.351	0.152	0.313	−0.0878	0.0381	−0.078

All displacements are in μm. The matrix set temperature = 820 C.

outer coatings on the fiber is slightly anisotropic with its stiff axis aligned in the fiber axial direction. The second outer coating is assumed to be isotropic and softer than SiC because of the presence of carbon. The third layer is similar, except that it is even softer because of the higher carbon content. The material properties of the titanium matrix and those of the SiC are chosen in the temperature range of 200–400 C. The set temperature for the titanium matrix and the fiber is below 900 C. Because of the possibility of time-dependent deformation we choose a slightly lower value, $T_6 = 820$ C. We assume that the current temperature is $T = 20$ C and the applied radial and axial stresses on the composite are zero.

The effective elastic properties listed in Table 3 for the successive layers are calculated by using (4)–(13c) in a recursive manner. For the outermost layer ($i = 6$), which corresponds to the titanium matrix, the effective shear moduli G_6^{Ae} and G_6^{Te} are calculated by using the expressions (A14)–(A21) in Appendix B for composites, rather than the concentric cylinder relations in (9) and (10). For comparative purposes, the bounds on the elastic constants are calculated by the recursive application of expressions (A22)–(A27), which assume that the inner phase is finely dispersed within the outer layer. These bounds are given in Table 4. The calculated values for the in-plane shear moduli from the recursive application of the Christensen's two-phase shear modulus in (A15)–(A21) are within the bounds given in Table 4.

The radial displacements and the axial strains are given in Table 5 at $T = 20$ C and $T = 1020$ C at the inner and the outer radii of each layer. The radial, hoop and axial stress

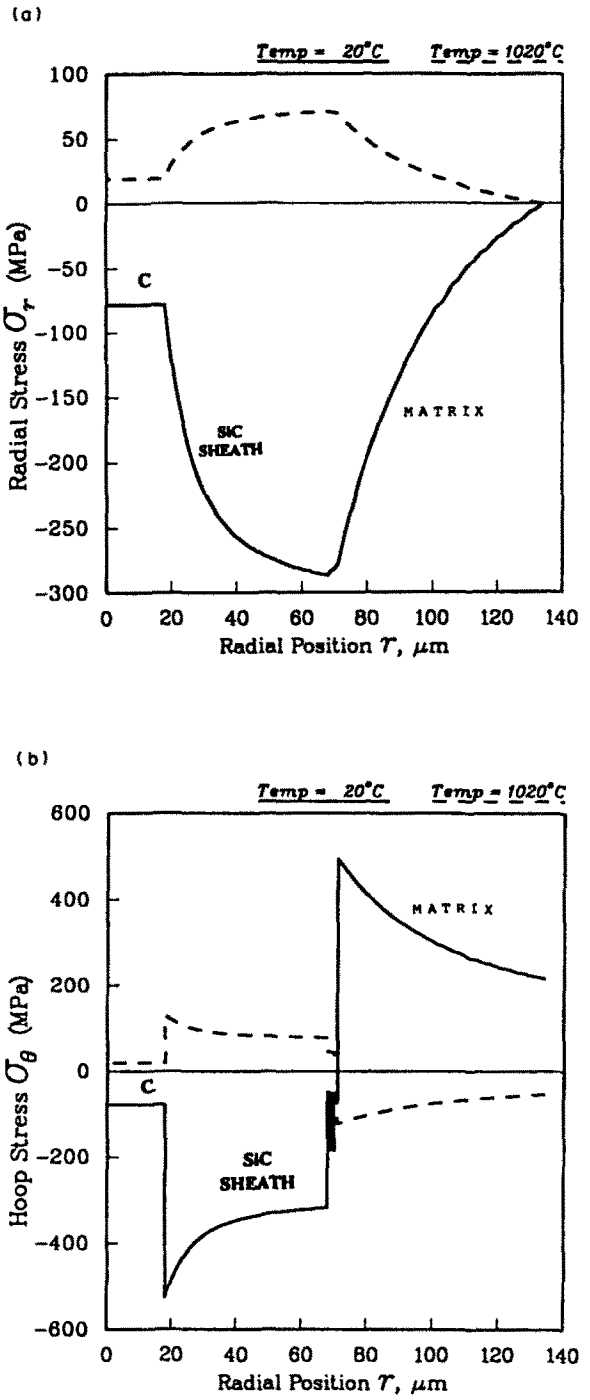

Fig. 4. The thermal stresses in the SiC fiber/Ti matrix composite as a function of the radial distance from the center of the fiber. The fibers are under axial compression whereas the matrix is in axial tension at room temperature. (a) Radial stress. (b) Hoop stresses. (c) Axial stresses. The elastic constants are assumed to remain constant over the temperature range 20–1020°C.

distributions, σ^{rr}, $\sigma^{\theta\theta}$ and σ^{xx}, are plotted as a function of the radial distance r in Figs. 4a–c. The predicted values for $T = 1020$°C may not be realistic because of the possibility of time-dependent deformation. The values for the radial displacements u_i^f and the axial strains in Table 5 have discontinuous values—with the exception of the interface between layers 1 and 2; however, this does not mean interface continuity is violated: see (29a). The discontinuity arises because the displacements are referred to the current temperature T, which is different than the "set" or "zero stress" temperatures T_i for the layers. The displacements

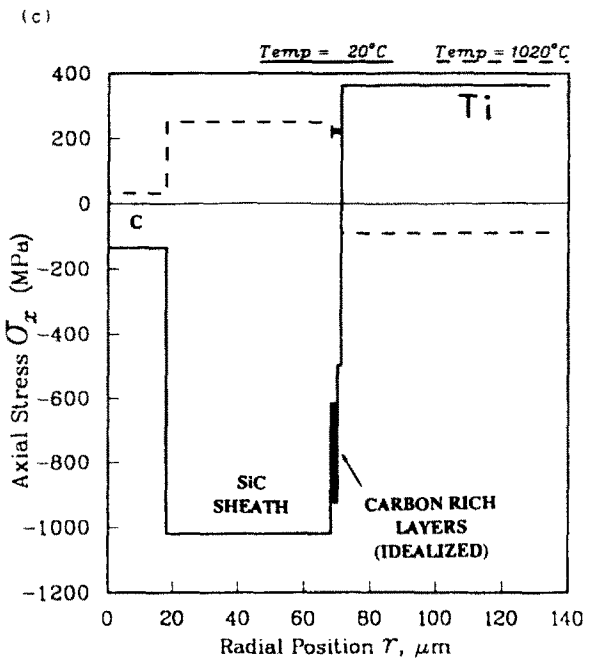

Fig. 4—*Continued.*

in Table 5 represent the actual displacements that the individual layers will undergo if all the layers are suddenly decoupled from one another at the current temperature T. These displacements are a measure of the amount of "shrink fit" between the layers at the current temperature T.

DISCUSSION

The presented recursive method can easily be converted into a computer algorithm to solve an arbitrary number of concentric cylinders. The model can be used to calculate five effective elastic constants and two thermal expansion coefficients of a uniaxially aligned composite which contains an arbitrary number of coatings on its fibers.

The validity of the recursive method can be ascertained in two ways. First, the predicted results from the recursive method can be compared with those obtained from the multiple-cylinder solutions, such as the ones given in Mikata and Taya (1985) and Pagano and Tandon (1988). The second method involves dividing one of the layers in an N-layer composite into two sublayers although the actual composite contains only N distinct layers. If the recursive method is to be exact, then the predicted results which are obtained with $N+1$ fictitious layers must be identical to those obtained by using N layers.

Application of both methods reveals that the stresses and the displacements calculated from the recursive method are exact for axisymmetric deformations that are independent of the axial direction. Furthermore, three of the elastic constants—the effective axial Young's modulus E^{Ac}, the axial Poisson's ratio ν^{Ac}, and the transverse bulk modulus k^{c}—and the two thermal expansion coefficients α^{Ac} and α^{Tc} can be calculated exactly for a uniaxial composite. However, as Table 6 shows, the effective axial and the shear moduli G^{Ac} and G^{Ts} cannot be calculated exactly. In Table 6, we tried to maximize the error which is represented by the difference in the values calculated using 6 and 7 layers. Actual error for the 6-layer composite is probably less. Dividing the layers further increases the error.

The expressions for the effective axial and the shear moduli G^{Ac} and G^{Tc} given by (9) and (10) are only approximately valid for replacing two concentric cylinders with a single homogeneous cylinder. These expressions are derived from a model that consists of two concentric cylinders embedded in an infinitely large medium that undergoes homogeneous deformation at infinite distance. All three phases are assumed to be transversely isotropic. The expressions given by (9) and (10) are determined by effectively replacing the inner two cylinders with a single transversely isotropic homogeneous cylinder, such that the stresses

Table 6. Check for accuracy of recursive method

		3 layers	4 layers	5 layers	6 layers	7 layers
G_i^{Te}	7-layer	79	78	78	76	44
	6-layer	114	111	111	105	47
G_i^{Ae}	7-layer	152	151	151	149	51
	6-layer	158	157	156	155	52

Layer 2 in Table 1 is divided into two parts at radius $r_2 = 43$ μm, so that the composite is regarded to consist of 7 layers, rather than 6. The material constants for the new layers 2 and 3 are identical. The predicted results by using 7 layers are identical to those given in Tables 3 and 5, except the values of the effective elastic constants G_i^{Te}, G_i^{Ae}, E_i^{Te} and v_i^{Te}. The estimated values for the effective shear moduli are given above in units of GPa. The difference represents error.

and the displacements in the infinite outer medium remain unchanged. It is expected that the recursive method will not be exact for general shear loading, since the expressions in (9) and (10) are derived under special loading situations.

The expressions for the effective axial and the shear moduli G^{Ae} and G^{Te} given by (9) and (10) are different than the expressions (A14)–(A27) derived for composites (see Appendix B) where the inner phase is assumed to be finely dispersed within the outer layer. In general, the predicted shear moduli from (9) and (10) are higher than the upper bounds for the composites, when the inner phase is stiffer than the outer phase. When the inner phase is more compliant, then the shear moduli for the concentric cylinders are lower than the lower bounds for a composite (compare the values provided in Table 3 and Table 4). It is possible to derive upper and lower bounds for the effective axial and the shear moduli G^{Ae} and G^{Te} for the recursive procedure. By using the bounds for the effective shear moduli it is possible to obtain limiting solutions for the microstresses and microstrains for nonaxisymmetric deformations. Recursive application of the lower bound for the shear moduli produces one limiting solution, whereas the upper bound value produces the other limiting solution. The difference between the predicted stress and displacements from the two cases represents the possible maximum error one may commit using the recursive method.

Although shear modulus measurements on the fibers are performed using torsion tests, the fibers inside a homogeneously deforming composite do not twist around their own axes. For a homogeneous transversely isotropic fiber, the shear modulus that is measured from a torsion test is the same as the fiber axial shear modulus G^A. However, for an inhomogeneous fiber the overall torsional modulus that is determined by a simple torsion test does not correspond to the effective axial shear modulus G^{Ae} for the cylinder assembly. The overall torsional shear modulus for any number of concentric cylinders can be determined by the recursive application of eqn (A28) in Appendix C. A relationship between the effective axial shear modulus G^{Ae} and the overall torsional shear modulus is established in Appendix C in terms of the relative volume fractions and the phase moduli.

The zero stress temperatures T_i for individual layers are not necessarily the same as the temperatures at which the layers are processed. The stresses that result from the processing, such as the deposition stresses and the thermal stresses, may be relieved because of time-dependent creep and relaxation. However, the residual stresses are not necessarily zero when the material reaches a limit temperature below which stress relaxation does not occur. If the magnitude of these residual stresses and the value of the limiting temperature are known, then it is possible to calculate a zero-stress temperature T_i for the layer i. However, the calculated value may not be a physically realizable temperature, such as above the melting point or below the absolute zero. The concept of zero-stress temperature, however, still retains its usefulness for calculating residual stresses in the layers, in the temperature range in which all constituents in the composite behave elastically.

When the layer properties vary with temperature or applied load—such as plastic deformation—the recursive method can be applied in an incremental manner for determining the stresses and the displacements. By successively adjusting the zero-stress temperatures T_i at each step, the layer stresses from the previous step can be generated as if

they were thermal stresses. The amount of initial stresses to be added to the right-hand side of the stresses in (22)–(24) is adjusted by varying the terms e^T and e^A. The corresponding zero-stress temperatures T_i are governed by (26a) and (26b).

Some other capabilities of the recursive method include the following:

(1) It can be shown that the recursive method can be applied accurately to concentric cylinders when there is radial temperature variation, provided that the deformations are axisymmetric and independent of the axial direction. Thus, it may not be necessary to solve the more complex four-concentric-cylinder model presented by Mikata and Taya (1985) for axisymmetric deformations.

(2) Weak interface coupling can be modeled by introducing a thin "soft" layer in the radial direction, i.e. by choosing the transverse Young's modulus much smaller than the axial modulus, $E^T \ll E^A$. The thickness of this thin layer should be chosen such that small variations in the chosen thickness value do not influence the stresses in the adjacent layers appreciably.

(3) The stresses and the displacements presented in this paper correspond to the applied traction boundary conditions. When homogeneous displacement boundary conditions are prescribed, then one can use the effective elastic properties of the composite prescribed in (4)–(10) to calculate the corresponding applied stresses. Subsequently, the recursive procedure described by eqns (14)–(34) can be applied to calculate the corresponding microstresses and the displacements.

(4) The expressions given by (6)–(13c) for the effective elastic constants of a two-concentric-cylinder assembly are valid when either one of the layers is made from an incompressible material. Incompressible materials are characterized by

$$\nu^A = 1/2, \quad \nu^T = 1 - E^T/2E^A, \quad k = \infty.$$

With the exception of the transverse bulk modulus k, the expressions (7)–(13c) for the effective elastic constants predict finite values when the transverse bulk moduli k_i or k_i^c approach infinity. The effective transverse bulk modulus for a two-concentric-cylinder assembly approaches infinity when both the inner and the outer cylinders are incompressible.

SUMMARY

The recursive method developed in this paper is capable of determining stresses and displacements in concentric cylinders under axisymmetric deformations, when all layers are linear elastic and there is interface continuity. Only two concentric cylinders are solved at each step. Applied axial and radial load as well as temperature change are considered. All the material properties are assumed to be transversely isotropic and uniform over the temperature range. Thermal stresses are properly accounted for by assuming that the set temperature is different for each constituent.

Three effective elastic constants—the axial Young's modulus E^{Ac}, the transverse bulk modulus k^c, and the axial Poisson's ratio ν^{Ac}—and the two thermal expansion coefficients α^{Ac} and α^{Tc} can be calculated exactly for a uniaxial composite that contains an arbitrary number of coatings on its fibers.

The remaining two effective elastic constants, the axial and the transverse shear moduli G^{Ac} and G^{Tc} cannot be determined exactly from the recursive method. The exact replacement of two concentric cylinders with a single cylinder is not possible under shear deformation. Approximate expressions are given in (9) and (10) for the axial and the in-plane shear moduli in order to replace two concentric cylinders with a single homogeneous cylinder. Comparison with the overall torsional shear moduli is made in Appendix C. More work is needed in order to estimate the error involved in using (9) and (10) in a recursive manner for computing nonaxisymmetrical elastic solutions.

The recursive method has been applied to a titanium matrix composite which is reinforced with heterogeneous SiC fibers. It is determined that the relatively compliant layer of carbon-rich external coating on the SiC fiber provides a gradual stress gradient across

the interface. This smooth transition reduces stress concentrations at the fiber matrix interface, thus preventing fiber failure.

Acknowledgements—Drs A. C. Kaya and C. A. Johnson at the GE Research and Development Center read the manuscript and made helpful suggestions. Dr P. A. Siemers provided discussions regarding the microstructure of the titanium matrix composite. The manuscript was typed by Paula Breslin.

REFERENCES

Brun, M. K. and Borom, M. P. (1989). Thermomechanical properties of CVD SiC filaments. *J. Am. Ceram. Soc.* **72**(10), 1993–1996.

Christensen, R. M. (1979). Mechanics of Composite Materials, pp. 84–89. Wiley, New York.

DiCarlo, J. A. (Private communication, 1990). NASA-Lewis Research Center.

Hashin, Z. (1979). Analysis of properties of fiber composites with anisotropic constituents. *J. Appl. Mech.* **46**, 543–550.

Lekhnitskii, S. G. (1981). Theory of elasticity of an anisotropic body, p. 231. MIR, Moscow.

Mikata, Y. and Taya, M. (1985). Stress field in a coated continuous fiber composite subjected to thermo-mechanical loadings. *J. Compos. Mater.* **19**, 554–578.

Mikata, Y., Takahashi, T., Su, S. K. and Uchida, Y. (1987). Development of functionalized materials using organometallic compounds IV. Thermal residual stresses during the fabrication of a Ni-coated continuous carbon fiber aluminum composites. *Bull. Chem. Soc. Jap.* **60**, 2593–2598.

Nimmer, R. P., Bankert, R. J., Russell, E. S. and Smith, G. A. (1989). Micromechanical modeling of fiber/matrix interface effects in transversely loaded SiC/Ti-6-4 metal matrix composites. *Proc. 13th Ann. Conf. on Composite Materials and Structures*, Jan. 18–20, 1989. NASA Langley.

Nutt, S. R. and Wawner, F. E. (1985). Silicon carbide filaments: microstructure. *J. Mater. Sci.* **20**, 1953–1960.

Pagano, N. J. (1972). The stress field in a cylindrically anisotropic body under two-dimensional surface tractions. *J. Appl. Mech.* **39**, 791–796.

Pagano, N. J. and Tandon, G. P. (1988). Elastic response of multidirectional coated fiber composites. *Compos. Sci. Technol.* **31**, 273–293.

Pagano, N. J. and Tandon, G. P. (1989). Thermo-elastic model for multidirectional coated fiber composites: Traction formulation. *Compos. Sci. Technol.* **38**, 247–269.

Siemers, P. A., Mehan, R. L. and Moran, H. (1988). A comparison of the uniaxial tensile and pure bending strength of SiC filaments. *J. Mater. Sci.* **23**, 1329–1333.

APPENDIX A

The quantities A, B, and C given in (10) for the effective transverse shear modulus G_i^{Te} are defined below in terms of the elastic properties and the volume fractions of the inner and the outer layers.

$$A = 4(\eta_1+1)A_0 + 2A_1(1-f_i)(G_{i-1}^{Te}/G_i^T - 1) + A_2(1-f_i)^2(G_{i-1}^{Te}/G_i^T - 1)^2 \tag{A1}$$

$$\frac{B}{f_i(\eta_1+1)} = 4(\eta_1+1)B_0 - 2B_1(G_{i-1}^{Te}/G_i^T - 1) + B_2(1-f_i)(G_{i-1}^{Te}/G_i^T - 1)^2 \tag{A2}$$

$$\frac{C}{4f_i^2(\eta_1+1)^2} = -C_1(G_{i-1}^{Te}/G_i^T - 1) + C_2(G_{i-1}^{Te}/G_i^T - 1)^2 \tag{A3}$$

$$\eta_1 = G_i^T/k_i \tag{A4}$$

$$\eta_2 = k_{i-1}^e/k_i \tag{A5}$$

$$A_0 = (\eta_1+\eta_2)[\eta_1+\eta_2+f_i\eta_1(\eta_2-1)(2\eta_1+3-f_i^2-2f_i^2\eta_1)] + f_i^4\eta_1^2(\eta_2-1)^2 \tag{A6}$$

$$\begin{aligned} A_1 = {} & (\eta_2-1)[2+8\eta_1+7\eta_1^2+\eta_2(2+3\eta_1)+f_i(8\eta_1^4+18\eta_1^3-8\eta_1-2+\eta_2(6\eta_1^3+13\eta_1^2+\eta_1-2)) \\ & +f_i^2(\eta_2(5\eta_1^2+13\eta_1+4)+2\eta_1^3(\eta_2-3)+4(\eta_1+1)^4)-f_i^3\eta_1(\eta_2(6\eta_1^2+7\eta_1+5)+2\eta_1(2\eta_1^2+\eta_1+1)) \\ & +f_i^4\eta_1^2(\eta_2-1)(1+2\eta_1)]+2(\eta_1+1)^2(1+2\eta_1)(1-f_i+2f_i^2) \end{aligned} \tag{A7}$$

$$\begin{aligned} A_2 = {} & (\eta_2-1)[(1+2\eta_1)(1+3\eta_1+\eta_2)+f_i(1+2\eta_1)(4\eta_1^3+6\eta_1^2-6\eta_1-2+\eta_2(2\eta_1^2+3\eta_1-2)) \\ & +f_i^2(10\eta_1^2+5\eta_1+1+\eta_2+4\eta_1\eta_2+4\eta_1(2\eta_1+\eta_2)(\eta_1+1)^2)-f_i^3\eta_1(1+2\eta_1)(2\eta_1\eta_2+\eta_2-2\eta_1)] \\ & +(1-f_i)^2(\eta_1+1)(1+2\eta_1)^2 \end{aligned} \tag{A8}$$

$$B_0 = \eta_1(\eta_2-1)(\eta_1+\eta_2)(1-f_i^2) \tag{A9}$$

$$\begin{aligned} B_1 = {} & 7\eta_1^2+10\eta_1\eta_2-4\eta_1^2(\eta_2-1)-\eta_2^2(3\eta_1^2+2\eta_1-4)+2f_i(\eta_1+\eta_2)[2\eta_1\eta_2-5\eta_1-3\eta_2+2\eta_1^2(\eta_2-1)] \\ & +4f_i^2(\eta_1+\eta_2)[\eta_2(1+\eta_1)+\eta_1^2(\eta_2-1)]-2f_i^3\eta_1(\eta_2-1)(\eta_1+\eta_2)(1+2\eta_1)+f_i^4\eta_1^2(\eta_2-1)^2 \end{aligned} \tag{A10}$$

$$B_2=(\eta_2+2\eta_1)[4(\eta_1+\eta_2)-(\eta_2-1)(\eta_1+2\eta_1^2)]+f_i(\eta_2+2\eta_1)[(\eta_2-1)(3\eta_1+2\eta_1^2)-2(\eta_1+\eta_2)]$$
$$+f_i^2[\eta_2+2\eta_1(\eta_2-1)][3\eta_1+4\eta_1^2+2\eta_2+3\eta_1\eta_2]-f_i^3\eta_1(\eta_2-1)[\eta_2+2\eta_1(\eta_2-1)] \quad \text{(A11)}$$

$$C_1=2\eta_1(\eta_2-1)(\eta_1+\eta_2)(1-f_i^2) \quad \text{(A12)}$$

$$C_2=f_i^2(\eta_1+\eta_2)[\eta_2+2\eta_1(\eta_2-1)]-\eta_1(\eta_2-1)(\eta_2+2\eta_1). \quad \text{(A13)}$$

APPENDIX B: THE EFFECTIVE AXIAL AND IN-PLANE SHEAR MODULI WHEN INNER PHASE IS FINELY DISPERSED

When the inner phase is finely distributed within the outer layer then eqns (9) and (10) (13b) for the shear moduli should be replaced by the expressions provided from Christensen (1979) and Hashin (1979) for the effective shear moduli of two-phase composites.

Axial shear modulus:

$$G_i^{Ae}=G_i^A\frac{G_i^A(1-f_i)+G_{i-1}^{Ae}(1+f_i)}{G_i^A(1+f_i)+G_{i-1}^{Ae}(1-f_i)}, \quad \text{(A14)}$$

Transverse shear modulus from Christensen (1979):

$$G_i^{Te}=G_i^T=(B+\sqrt{B^2-4AC})/(2A) \quad \text{(A15)}$$

where

$$A=3f_i(1-f_i)^2(\eta_1-1)(\eta_1+\eta_2)+[\eta_1\eta_3+\eta_2\eta_3-(\eta_1\eta_3-\eta_2)f_i^3][f_i\eta_1(\eta_1-1)-(\eta_1\eta_3+1)] \quad \text{(A16)}$$

$$B=-3f_i(1-f_i)^2(\eta_1-1)(\eta_1+\eta_2)+\tfrac{1}{2}[\eta_1\eta_3+(\eta_1-1)f_i+1][(\eta_1-1)(\eta_1+\eta_2)-2(\eta_1\eta_3-\eta_2)f_i^3]$$
$$+\frac{f_i}{2}(\eta_3+1)(\eta_1-1)[\eta_1+\eta_2+(\eta_1\eta_3-\eta_2)f_i^3] \quad \text{(A17)}$$

$$C=3f_i(1-f_i)^2(\eta_1-1)(\eta_1+\eta_2)+[\eta_1\eta_3+(\eta_1-1)f_i+1][\eta_1+\eta_2+(\eta_1\eta_3-\eta_2)f_i^3] \quad \text{(A18)}$$

$$\eta_1=G_{i-1}^{Te}/G_i^T \quad \text{(A19)}$$

$$\eta_2=1+2G_{i-1}^{Te}/k_{i-1}^{Te} \quad \text{(A20)}$$

$$\eta_3=1+2G_i^T/k_i. \quad \text{(A21)}$$

The recursive expression for the single-valued transverse shear modulus in (A15)–(A21) is the modified version of the expression provided by Christensen, as explained previously (see (1a–c)). We extracted the physically meaningful root from the quadratic given in Christensen in order to arrive at (A15). The value of G_i^{Te} provided by (A15) is always in between the upper bound value G_i^{TeH} and the lower bound G_i^{TeL} (Hashin, 1979) which are given below. A superscript "H" is used to denote an upper bound, and "L" to denote a lower bound. Both the upper and the lower bounds G_1^{TeH} and G_1^{TeL} are initially set to the in-plane shear modulus G_1^T of the innermost core.

Case (i)

If $k_{i-1}^{Te}>k_i$; $G_{i-1}^{TeH}>G_i^T$, then

$$G_i^{TeL}/G_i^T=1+\frac{2f_i(G_{i-1}^{TeL}-G_i^T)(k_i+G_i^T)}{2G_i^T(k_i+G_i^T)+(1-f_i)(k_i+2G_i^T)(G_{i-1}^{TeL}-G_i^T)} \quad \text{(A22)}$$

$$G_i^{TeH}/G_i^T=1+\frac{(1+\beta_i)f_i}{\rho-f_i\left(1+\dfrac{3\beta_i^2(1-f_i)^2}{\alpha f_i^3+1}\right)} \quad \text{(A23)}$$

$$\varkappa = \frac{\beta_1 - \gamma\beta_2}{1+\gamma\beta_2}; \quad \rho = \frac{\gamma+\beta_1}{\gamma-1}; \quad \gamma = G_{i-1}^{\mathrm{TeH}}/G_i^{\mathrm{T}}; \quad \beta_1 = k_i/(k_i+2G_i^{\mathrm{T}}); \quad \beta_2 = k_{i-1}^{e}/(k_{i-1}^{e}+2G_{i-1}^{\mathrm{TeH}}). \tag{A24}$$

Case (ii)

If $k_{i-1}^{e} < k_i$; $G_{i-1}^{\mathrm{TeL}} < G_i^{\mathrm{T}}$, then

$$G_i^{\mathrm{TeH}}/G_i^{\mathrm{T}} = 1 + \frac{2f_i(G_{i-1}^{\mathrm{TeH}} - G_i^{\mathrm{T}})(k_i + G_i^{\mathrm{T}})}{2G_i^{\mathrm{T}}(k_i+G_i^{\mathrm{T}}) + (1-f_i)(k_i+2G_i^{\mathrm{T}})(G_{i-1}^{\mathrm{TeH}} - G_i^{\mathrm{T}})} \tag{A25}$$

$$G_i^{\mathrm{TeL}}/G_i^{\mathrm{T}} = 1 + \frac{(1+\beta_1)f_i}{\rho - f_i\left(1 + \dfrac{3\beta_1^2(1-f_i)^2}{\varkappa f_i^3 - \beta_1}\right)}. \tag{A26}$$

The quantity β_1 is given in (A24). The new values for the quantities $\varkappa$, ρ, β_2, γ are calculated from (A24) by replacing the superscript "H" with "L". Thus, the new values of γ and β_2 are governed by

$$\gamma = G_{i-1}^{\mathrm{TeL}}/G_i^{\mathrm{T}}; \quad \beta_2 = k_{i-1}^{e}/(k_{i-1}^{e}+2G_{i-1}^{\mathrm{TeL}}). \tag{A27}$$

APPENDIX C: TORSIONAL SHEAR MODULUS FOR TWO CONCENTRIC CYLINDERS

For the replacement of two concentric cylinders with a single transversely isotropic homogeneous cylinder, the effective axial shear modulus G_i^{Ae} is calculated from (9). However, the calculated G_i^{Ae} is not the overall shear modulus that can be measured from a torsion test performed on the two-cylinder assembly. The measured torsional shear modulus would be identical to the axial shear modulus G_i^{Ae} for a solid homogeneous cylinder. Assuming shear strain continuity at the interface, the overall torsional shear modulus for two concentric cylinders is given by

$$G_{i,\mathrm{Torsional}}^{\mathrm{Ae}} = G_i^{\mathrm{A}} + f_i^2(G_{i-1,\mathrm{Torsional}}^{\mathrm{Ae}} - G_i^{\mathrm{A}}). \tag{A28}$$

The effective axial shear moduli for the innermost fiber ($i = 1$) are the same and equal to the axial shear modulus of material 1,

$$G_1^{\mathrm{Ae}} = G_{1,\mathrm{Torsional}}^{\mathrm{Ae}} = G_1^{\mathrm{A}}. \tag{A29}$$

Using the measured value of $G_{N,\mathrm{Torsional}}^{\mathrm{Ae}}$ from a torsion test on an N-layered cylinder, the torsional shear moduli $G_{i,\mathrm{Torsional}}^{\mathrm{Ae}}$ for successive numbers of inner layers i can be calculated from (A28) in a recursive manner. Upon reaching the innermost layer ($i = 1$), the recursive relationship in (9) is used to calculate the effective axial shear moduli G_i^{Ae} for any number of layers i. With this procedure, the effective axial shear moduli can be calculated from experimentally observed values of the overall torsional shear moduli.

When only two concentric cylinders are present ($N = 2$), then the relationship between the effective axial and the torsional shear moduli is governed by

$$\frac{G_2^{\mathrm{Ae}} - G_{2,\mathrm{Torsional}}^{\mathrm{Ae}}}{G_1^{\mathrm{A}} - G_2^{\mathrm{A}}} = 2f_i/(1+f_i) - f_i^2 \tag{A30}$$

where f_i denotes the volume fraction of the inner ($i = 1$) cylinder, and G_1^{A} and G_2^{A} are the axial shear moduli for the inner and the outer cylinders, respectively. The right-hand side of (A30) vanishes for $f_i = 0$ and $f_i = 1$, and assumes a maximum value of 0.42 at $f_i = 0.46$.